Thermodynamic and hydrodynamic peculiarities of a foam lamella confined in a cylindrical pore

Konstantin Kornev[1] and Galina Shugai,[2]
[1]*The Institute for Problems in Mechanics, Russian Academy of Sciences, Prospect Vernadskogo 101, Moscow 117526, Russia*
[2]*Department of Hydraulic Engineering, The Royal Institute of Technology, 100 44 Stockholm, Sweden*
(Received 12 May 1998)

The paper investigates a specific behavior of foam films: lamellae confined in a cylindrical prewetted pore. Since both the lamella and wetting film are ultrathin (<100 nm), classical thermodynamics is generalized to account for the effects of intermolecular forces. The conditions of coexistence of a lamella and wetting films are established. The problem of lamella motion is considered as a free boundary problem. The theory predicts three sliding regimes, depending on the priority of viscous, long-range surface, and capillary forces. At low speeds, the long-range surface, and capillary forces dominate the viscous one. The friction force acting on the lamella is then proportional to the speed. The pressure drop required to keep the lamella moving can be of the same order of magnitude as the critical pressure drop for lamella rupture. [S1063-651X(98)07112-8]

PACS number(s): 82.70.Rr, 68.10.−m, 68.90.+g

I. INTRODUCTION

The problem of foam transport in porous media has received a great deal of attention in the previous decades due to the unique ability of foams to reduce the gas flux through the medium [1,2]. Two main mechanisms of this reduction have been proposed. The first is attributed to a specific action of the capillary forces, which leads to the blockage of the gas paths by the foam films (or lamellae). As a result, the permeability to gas is reduced up to several orders of magnitude compared to that for the corresponding gas-liquid system without a foaming agent. In addition to a reduction of the permeability, foams radically change the rheological behavior of the gas phase [1–3]. The conventional point of view on the effect originates from a work by Bretherton [4], in which he explained the mechanism of the nonlinear friction of a bubble as a result of the competition between the capillary and viscous forces. In particular, he showed that the expected extra-pressure drop ΔP additional to the Laplacian capillary pressure, increases with the bubble speed to the $\frac{2}{3}$ power. Hirasaki and Lawson [5], and some others (e.g., Refs. [1,6]), applied the Bretherton approach to bubble train motion through smooth capillaries and bead packs. They assumed, though implicitly, that the foam flow is similar to the motion of a hypothetical single-phase system. Thus the joint motion of the gas, liquid slugs separating the isolated bubbles, and the wetting film coating the pore walls is treated by means of the so-called pseudohomogeneous Darcy flow model that prescribes an *a priori* relation between the applied pressure gradient and the resulting flow rate. Within this approach, there is no relative motion of foam lamellae, and every bubble moves in unison with others. However, the average velocities of different phases can be distinguished. In particular, the steady velocity of the gas bubble is determined by the average velocity of the faster flowing fluid near the center of the lamella (or liquid lens). Then the volume swept out by a long bubble moving at a constant speed U can be estimated by the product of the average speed of the liquid and the cross-sectional area of the lining film. The estimation reveals that the average speed of the wetting fluid is less than the bubble velocity, even though the difference is slight. The reduction in apparent gas viscosity, however, can be significant because the viscosity of the wetting fluid is much larger than that of the gas.

The other model of the foam flow through a capillary is based on the wavelike motion of lamellae [7]. For each lamella in the train, the physical picture of the flow resembles a flow generated by a sail boat. Thus the model is called the sail boat model. The lamella draws a meniscus (the Plateau border), so that a lubrication flow occurs within both the meniscus and the respective wetting films. The lamella serves as a sail, thus forcing the wetting film to move. Similarly to the Bretherton scheme, the main flow patterns are concentrated within the wetting film. However, the lamella thickness, its radius of curvature, and the lamella tension may depend on the changes within the wetting film. Therefore, the law of lamella motion cannot be predicted in advance, since collective phenomena drive the dynamics of each lamella. Lamellae can move steadily only under certain restrictions on pressure distribution within the train.

The above described schemes of foam friction seem to operate with different objects; the first one deals with the bubble as a whole, while the second one treats each lamella independently. However, from the mathematical point of view, both schemes deal with foam lamellae rather than the discrete bubbles. In spite of the sufficiently conventional division, the distinctions should be stressed, because they imply different mechanisms of foam transport in porous media. In particular, the first scheme is implicitly associated with the creep of the bubble train as a whole, while the second treats the foam motion as a wavelike displacement of lamellae in caravans.

The main goal of this paper is to clarify the nature of lamella sliding through a smooth capillary. Though in earlier papers one of us put forward the physical idea underlying the sail boat model [7], no mathematical formulation has been presented. To our knowledge, the only work that utilizes elements of the sail boat model is that presented by Ida and Miksis [8]. However, they were interested in the lamella thinning phenomena, and postulated *a priori* the linear Newtonian friction law for the lamella. The present study is aimed at the physical picture of the lamella slippage.

The relative intensity of viscous and capillary forces can be expressed in terms of the capillary number $\mathrm{Ca}=\mu U/\sigma$, in which μ is the fluid viscosity, U is the lamella velocity, and σ is the surface tension. In most applications, the values of the capillary number are very small; for example, assuming that the typical seepage speed is $U\approx 1$ cm/day, one obtains $\mathrm{Ca}\approx 10^{-8}$ for aqueous foams with $\mu\approx 10^{-3}$ Pa s, $\sigma \approx 0.03$ N/m. We confine ourselves to this case in the present paper. It is a known fact that the Bretherton theory is unable to reproduce the characteristic feature of the wetting films dynamics in this range of capillary numbers [4,9,10]. Because of the mathematical similarity of the Bretherton problem and the problem of lamella motion, one may expect a discrepancy between the theory and experimental data on the lamella resistance. Actually, Hirasaki and Lawson [5] demonstrated experimentally that even in the range of capillary numbers appropriate for the Bretherton theory, the pressure drop per foam bubble is about one order of magnitude larger than that predicted by the theory. They attributed this discrepancy to the effect of the surface tension gradient that is caused by a specific redistribution of the surfactant over the interface. Later on, this hypothesis was assessed theoretically by Herbolzheimer [11] and Chang and Ratulowski [12]. They assumed the solution to be dilute, and obtained an extra pressure drop only $4^{2/3}$ times the Bretherton expression. Therefore, the anomalous extra pressure drop observed by Hirasari and Lawson cannot be explained by the surface tension gradient only.

Although the scope of the reasoning for the discrepancy between the Bretherton theory and his experiment on a single bubble has been extended, all the explanations have always been attributed to the ordinary lubrication approximation. The explanations include wall roughness [13], instability of the meniscus [4], and adsorbed impurities [4,14,15].

Teletzke [14] was the first to point out the significance of long-range molecular forces when the meniscus extends to a film of a very small thickness (1 μm or less). He treated the displacement of an individual bubble in a quasistatic regime, and augmented Bretherton's theory by including the disjoining pressure that serves as a force per unit area additional to ordinary pressure [16]. The concept of disjoining pressure allows one to use conventional hydrodynamic variables and, at the same time, to account for double-layer electrostatic forces and the like inherent to an ultrathin film. Teletzke resolved Bretherton's enigmatic assertion that the thickness of the deposited film is independent of the substrate wettability and diminishes as the capillary number approaches zero. In particular, he showed that the film thickness levels off to an equilibrium value at the limit of negligibly small capillary numbers. Chen [13] confirmed Teletzke's prediction by measuring the thickness of film surrounded by air bubbles and oil drops in water. We select the case of ultrathin wetting films, because of its basic importance in the treatment of the problem of the foam friction at very low speeds.

The foam resides in a porous medium as a gas-liquid mixture: a continuous liquid phase wetting the rock and the gas that is made discontinuous by lamellae. The wetting films on the pore walls of varying curvature link the menisci in the corners of cusped pores, hence the films are forced to have a varying thickness in order to balance the capillary pressure by their disjoining pressure. If the rock is not wetted, the liquid phase is accumulated at the pore corners or forms discrete droplets. However, this situation is rare, since the presence of surfactant improves the wettability [16,17]. Thus we consider only wet capillaries.

In Sec. II, we discuss thermodynamic peculiarities of free-standing lamella. Because of its unique structure, the lamella serves as a thermodynamic phase; therewith, it senses what happens in the wetting film. As a result, in confining systems such as pores, the conditions of equilibrium coexistence of an individual lamella and the wetting film prove to be specific. The thermodynamic model is further generalized to account for the hydrodynamic feature of the lamella motion. In Sec. III, we formulate the sail boat model of lamella sliding. Then we consider a traveling wave solution in Sec. IV. The solution possesses a rather wide spectrum of admissible regimes of lamella motion. The regimes depend on the priority of the forces that influence the lamella motion. In the regime of small capillary numbers, the shape of the Plateau border is almost entirely controlled by the capillary and surface forces. This is the so-called quasistatic regime of lamella creep. In accordance with the ordinary approach to the calculation of the transport coefficients [18], we are interested in small perturbations of the thermodynamic characteristics of the wetting film. We show that the lamella velocity depends linearly on the pressure drop across the lamella. The friction coefficient is affected by the physicochemical properties of the pair ''wetting film plus substrate'' via the disjoining pressure isotherm.

II. WHY A LAMELLA DIFFERS FROM A LENS. FREE-STANDING LAMELLA

Prior to analyzing the mechanism of lamella friction, we briefly review the thermodynamic conditions that elucidate the distinction between a lamella and liquid lens. The analysis of the lamella equilibrium in a bulk foam is well known, and it has an elegant solution in the form of Plateau's law [19]. However, the simple case of a lamella spanning a wetted pore appears to have been nondeveloped. At the same time, such a case could clarify the role of substrate wettability and its influences on the foam stability.

To explain the distinctions between a lamella and liquid lens, it is useful to recall general micromechanical features of the lamella formation [20,21]. A foam lamella forms in two stages. The first one is the creation of a lens. The wetting film coating the capillary snaps off and transforms into a lens when the film thickness exceeds a certain value [22,23]. Then, under the Laplacian capillary pressure, a lens squeezes liquid away until its interfaces touch each other. At this moment, a lens that contains a pure liquid immediately disappears. However, if a surfactant is present, a lens with adjoint interfaces can be stable. A stable lamella may form as the result of the transition from the bulk solution to an interesting thermodynamic state. Owing to the effects of the lamella disjoining pressure $\Pi_l(h_l)$, the effective tension 2γ of a lamella differs from the sum 2σ of the tensions of its two interfaces with the surrounding gas. Thus the tension has the form [16,24].

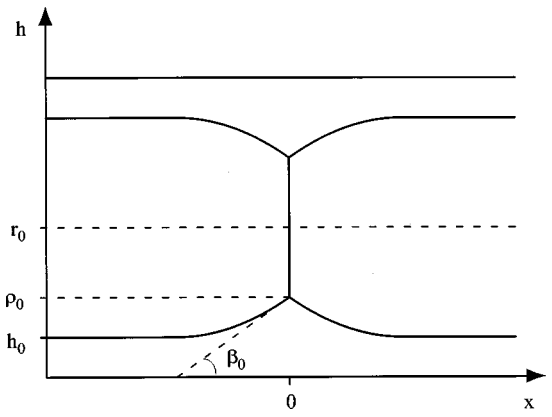

FIG. 1. Free-standing lamella confined in a cylindrical capillary.

$$2\gamma = 2\sigma_f + \Pi_l(h_l)h_l = 2\sigma + \int_{h_l}^{\infty} \Pi_l(h)dh + \Pi_l(h_l)h_l, \tag{1}$$

where σ is the ''bare'' surface tension, and σ^f is the effective surface tension.

The force balance at the junction between the Plateau border and lamella thus requires a finite contact angle [25]. The contact angles are typically small, ranging from somewhat less than 1° to a few degrees (see, for a review, Refs. [26, 27]). It is recognized, however, that they are responsible for the patterning in bulk foams [28]. The question naturally arises to what extent the substrate wettability influences the equilibrium property of a lamella.

To clarify this question, we consider the somewhat simplified thermodynamic model of the lamella formation. Our basic hypothesis is that the characteristic height of the Plateau border is much greater than the characteristic size of the transition zone between the lamella and meniscus (Fig. 1). Usually, the pore size r_0 is of the order of 100 μm, and the transition zone between the flat lamella and Plateau border is assessed as $l \sim 1$ μm [29]. Therefore, the contact conditions of the lamella and meniscus can be modeled by introducing a sharp contact line with the associated contact angle $\pi - 2\beta_0$, at which liquid-air interfaces meet [25]. In the following treatment, we consider the so-called regime of *pseudopartial wetting* [16,30]. The regime is termed ''pseudo'' because the solid is completely coated with a film of the thickness h, but, at the same time, the meniscus could form a finite apparent contact angle. Since the radius of action of the lamella is small compared with the height of the Plateau border, we assume that the wetting film senses only the disjoining pressure caused by the substrate. An analysis of the equilibrium condition for pores comparable with the thickness of transition zone ($r_0 \sim l$) is beyond the scope of our paper.

The equilibrium shape of the meniscus, for example, of its left branch can be obtained by integrating the augmented Young-Laplace equation

$$\frac{\sigma h''}{(1+h'^2)^{3/2}} + \frac{\sigma}{(r_0-h)(1+h'^2)^{1/2}} = P_g - P_w - \Pi(h) \tag{2}$$

together with the boundary conditions

$$h'|_{x=-\infty} = 0 \tag{3}$$

at infinity, and

$$h'|_{x=-0} = \tan \beta_0 \tag{4}$$

at the contact line.

In Eq. (2), P_g and P_w are the gas and fluid pressures, respectively, $\Pi(h)$ is the disjoining pressure, σ is the surface tension, and a prime denotes the derivative with respect to x. At infinity, we have a uniform film of the thickness h_∞. Hence the following equation holds:

$$\frac{\sigma}{(r_0-h_\infty)} + \Pi(h_\infty) = P_g - P_w. \tag{5}$$

The contact angle β_0 cannot be presumed as a physical constant, since it is affected by the capillary pressure. More precisely, the force balance at the contact line, where the lamella meets the meniscus, takes the form

$$2\sigma \sin \beta_0 = 2\gamma = 2\sigma + \int_{h_l}^{\infty} \Pi_l(h)dh + \Pi_l(h_l)h_l. \tag{6}$$

Sometimes, the equation is modified by adding a term with a line tension [25,29]. The model with a line tension is aimed at implicit consideration of the effect of the transition zone between the meniscus and flat lamella. The transition zone, however, can be correctly taken into account by the technique of matching asymptotic expansions [31]. We focus on the transition zone between the meniscus and wetting film, because it plays the key role in hydrodynamics. In the thermodynamic equilibrium, the disjoining pressure in the lamella equals the capillary pressure

$$\Pi_l(h_l) = P_g - P_w = \frac{\sigma}{(r_0-h_\infty)} + \Pi(h_\infty). \tag{7}$$

Hence the contact angle senses what happens in the wetting film far from the contact line.

The equilibrium shape of the meniscus can be found explicitly by expressing the Young-Laplace equation via the cosine of the current inclination angle of the profile [32]

$$\cos \beta(h) = (1+h'^2)^{-1/2}. \tag{8}$$

Then Eq. (2) takes the form

$$-\frac{d \cos \beta(h)}{dh} + \frac{\cos \beta(h)}{(r_0-h)} = \frac{P_g - P_w}{\sigma} - \frac{1}{\sigma}\Pi(h), \tag{9}$$

and the boundary conditions (3) and (4) give

$$\cos \beta(h_\infty) = 1, \tag{10}$$

$$\cos \beta(\rho_0) = \cos \beta_0. \tag{11}$$

Integrating Eq. (9) together with the boundary conditions (10) and (11), we arrive at the formula for the crest height

$$\frac{(P_g-P_w)}{2\sigma}(2r_0-\rho_0-h_\infty)(\rho-h_\infty)$$

$$=\frac{1}{\sigma}\int_{h_\infty}^{\rho_0}(r_0-h)\Pi(h)dh+(r_0-h_\infty)-(r_0-\rho_0)\cos\beta_0. \tag{12}$$

It is useful to rewrite Eq. (12) in its customary form [25,33] by introducing the apparent contact angle θ as

$$\cos\theta=1+\frac{1}{\sigma}\int_{h_\infty}^{\rho_0}\frac{(r_0-h)}{r_0}\Pi(h)dh+\frac{h_\infty^2}{2r_0(r_0-h_\infty)}$$

$$+\frac{1}{2\sigma}\Pi(h_\infty)h_\infty\left(2-\frac{h_\infty}{r_0}\right). \tag{13}$$

Then Eq. (12) takes the following familiar form [25,33]:

$$\frac{(P_g-P_w)}{2\sigma}r_0(1-\vartheta^2)=\cos\theta-\vartheta\cos\beta_0, \tag{14}$$

where

$$\vartheta=\frac{(r_0-\rho_0)}{r_0}.$$

In the limiting case $\rho_0/r_0\ll 1$, or in the two-dimensional case, Eqs. (13) and (14) give

$$\cos\theta=1+\frac{1}{\sigma}\int_{h_\infty}^{\rho_0}\Pi(h)dh+\frac{1}{\sigma}\Pi(h_\infty)h_\infty, \tag{15}$$

$$P_g-P_w=\frac{\sigma}{\rho_0}(\cos\theta-\cos\beta_0). \tag{16}$$

In particular, Eq. (16) is merely the Young-Laplace equation written for an apparent interface, provided that the interface is modeled by an arch [Fig. 2(a)]. The range of applicability of Eq. (15) is restricted to the film thickness, ensuring the existence of an apparent contact angle. Thus, the inequality $\theta\geqslant 0$ must hold. In the opposite case, the meniscus does not intersect the capillary wall and the apparent contact angle loses its meaning [Fig. 2(b)]. However, even in such a case, Eq. (16), holds and allows one to assess the effect of the substrate wettability on the thermodynamic characteristics of a confined lamella. In the theory of wetting of pure liquids, a similar modification of the Young-Laplace equation was pointed out a long time ago, and now the existence of a prolonged transition zone provides a useful tool for measuring the disjoining pressure isotherms and related characteristics (for a review, see Ref. [34]).

Using the assumption that the meniscus crest is much higher than the film thickness, and the crest is much smaller than the radius of capillary, we may consider only the asymptotic profile of the Plateau border. The profile is obtained by integrating Eq. (9) in the limiting case $r_0\to\infty$,

$$\cos\beta(h)=\frac{1}{\sigma}\int_{h_\infty}^{h}(\Pi(t)-\Pi(h_\infty))dt+1. \tag{17}$$

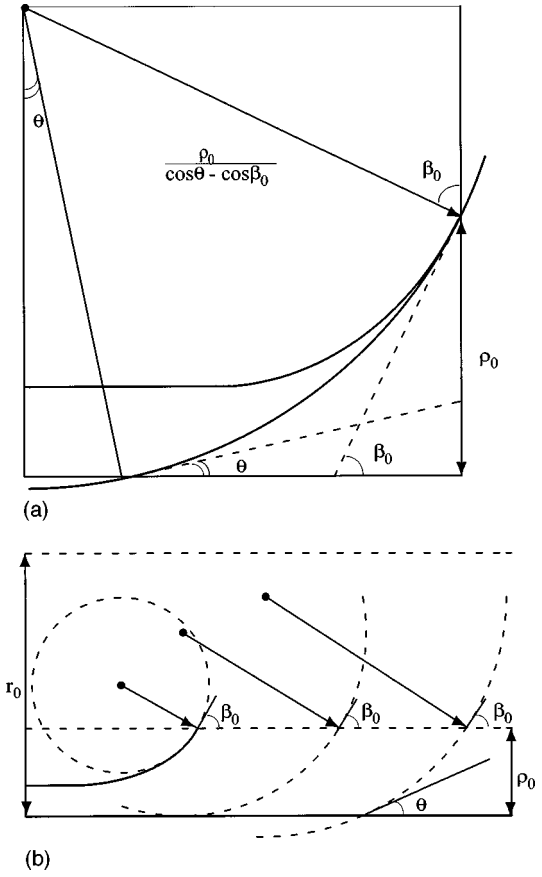

FIG. 2. (a) Geometrical construction elucidating the generalized Young-Laplace equation (16). (b) The apparent contact angle loses its physical meaning if the apparent radius of the Plateau border is smaller that a certain value.

It should be noted that the resulting profile has been presented by several authors in different forms, for example, Refs. [35,23,32,36]. Thus the Plateau border has the form

$$x=\int_{\rho_0}^{h}\left(\left(\cos\beta_0-\frac{\int_h^{\rho_0}(\Pi(h)-\Pi(h_\infty))dh}{\sigma}\right)^{-2}-1\right)^{-1/2}dh. \tag{18}$$

In particular, for any disjoining pressure isotherm of the form $\Pi(h)=A_n/h^n$ with an integer n, the size of the transition region can be estimated as $l_{pl}\sim\sqrt{\rho_0 h_\infty/(1-\cos\beta_0)n}$ (see the Appendix). In this respect, the size of the Plateau borders of lamellae created from different frothing solutions are indistinct, provided that the physical parameters ρ_0 and h_∞ are identical.

Concluding the results of this section, we emphasize that for a confining lamella, the conditions of thermodynamic equilibrium depend on the wettability conditions for the substrate. Hence the conditions must be taken into account in the analysis of the lamella friction.

III. HYDRODYNAMICS OF LAMELLA SLIPPAGE. SAIL BOAT MODEL

In the thermodynamic equilibrium, the contact conditions between a free film and a wetting film can be found by applying ordinary thermodynamic rules. The case of moving

lamella dictates rules. The flow pattern within the wetting film and lamella plays an important role here. In the motion, all geometrical parameters such as the lamella thickness, wetting film thickness, inclination angles, and curvatures of the menisci at the Plateau border altogether must be mutually consistent. From the hydrodynamic point of view, the lamella causes a time-dependent tensile force applied to the wetting film surface. Therefore, from the mathematical point of view, the problem of determination of the shape of the moving wetting film can be considered as a free boundary problem. Thus the thickness of the wetting film behind and ahead of the contact line, and the time-dependent coordinates of the contact line, must be determined. This should be done by accounting for the specific features of the coexistence conditions of the free film and the wetting film.

The problem requires the solution of the respective hydrodynamic problem for the wetting fluid, which can be a difficult task. However, the lubrication approximation of the flow pattern can be utilized instead. While not precise, it often provides correct trends [4,10,30,37–39]. Thus, neglecting the gas viscosity and assuming that pressures within the bubbles are constants, the volumetric flow rate can be written as

$$q=-\frac{h_i^3}{3\mu}\frac{\partial P_w}{\partial x}, \tag{19}$$

where μ is the viscosity of the wetting fluid, $h_i(i=\pm)$ is the film thickness in each bubble, and x is the coordinate along the capillary. At each point, the pressure P_w across the film is a constant that depends on the film thickness as follows:

$$P_w=P_i-2\sigma_i H-\Pi(h_i), \tag{20}$$

where P_i is the gas pressure within the ith bubble, σ_i is the surface tension in the ith bubble, and $2H$ is the curvature of the interface. Hereinafter, we consider the limiting case $h/r_0\ll 1$. Then the curvature can be expressed as

$$2H=\frac{d^2h_i}{dx^2}\Big/\left(1+\left(\frac{dh_i}{dx}\right)^2\right)^{3/2}. \tag{21}$$

The presence of the disjoining pressure $\Pi(h_i)$ guarantees the film stability. Thus, the flow within the film is controlled by the ''dynamic'' capillary pressure, and it tends to an equilibrium between the capillary, surface, and viscous forces. For example, if the pushing force is switched off, the bubble profile works out the shape of constant mean curvature, as Eqs. (20) and (21) predict.

The condition of mass balance provides the final connection between the pressure and film thickness:

$$\frac{\partial h_i}{\partial t}+\frac{\partial q}{\partial x}=0. \tag{22}$$

Thus Eqs. (19)–(22) give two film profiles h_- and h_+ associated with the left and right bubbles, respectively. The profiles have to be matched at the three-phase contact line. At the free boundary, i.e., at the three-phase contact line, five boundary conditions should be formulated because the curvature in Eq. (20) is expressed by means of the second derivatives of the fields, and Eqs. (19) and (22) add two more derivatives.

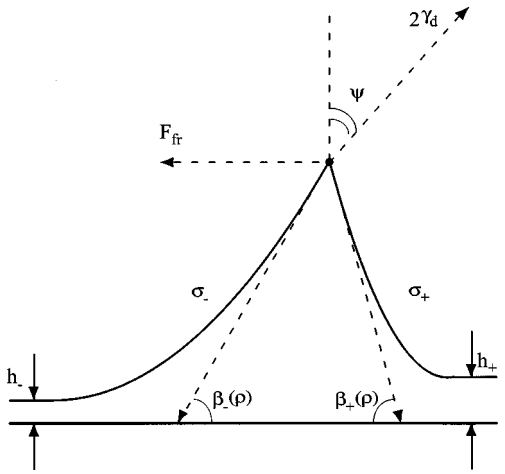

FIG. 3. Schematic of a lamella sliding over the wetting film.

(a) Continuity condition. The first boundary condition is the continuity condition, namely,

$$h_-|_{x=\xi-0}=h_+|_{x=\xi+0}=\rho, \tag{23}$$

where ξ is the contact line position.

(b) Force balance. The usual conditions of local mechanical equilibrium give the second boundary condition. However, some restrictions due to the geometry appear (Fig. 3). We denote by β_i $(i=\pm)$ the inclination angle of the ith air-wetting fluid interface with respect to the rigid wall. Since the profile of the ''minus'' film is described by an increasing function, and the ''plus'' film by a decreasing one, the angles β_i are expressed as

$$\tan\beta_-(\rho)=\left.\frac{\partial h_-}{\partial x}\right|_{x=\xi-0}, \tag{24}$$

$$\tan\beta_+(\rho)=-\left.\frac{\partial h_+}{\partial x}\right|_{x=\xi+0}. \tag{25}$$

Thus Eqs. (24) and (25) connect the inclination angles with the first spatial derivative, i.e., with the slope of the film profiles at the contact line. On the other hand, the inclination angles depend on the lamella tension, as follows from the conditions of mechanical equilibrium:

$$\sigma_-\cos\beta_-(\rho)-\sigma_+\cos\beta_+(\rho)=2\gamma_d\sin\psi-F_{\rm fr}, \tag{26}$$

$$\sigma_-\sin\beta_-(\rho)+\sigma_+\sin\beta_+(\rho)=2\gamma_d\cos\psi, \tag{27}$$

where $2\gamma_d$ is the dynamic tension of the lamella, and $F_{\rm fr}$ is the extra force caused by a specific friction of the contact line. The value of this force is unknown beforehand, and it must be found.

The surface tensions in adjacent bubbles can be distinguished by virtue of different dynamic concentrations of the surfactant. However, if we neglect the concentration effect, then the surface tensions in different bubbles do not differ. As shown in Sec. II, the equilibrium lamella tension is a function of the film thickness. However, the dynamic lamella tension differs from its thermodynamic value due to a contribution from the hydrodynamic flow within the lamella.

(c) Lamella thickness and dynamic tension. We assume for simplicity that, during the motion, the lamella bulges uniformly like a spherical cap and does not change its volume; the fluid is redistributed over a new area due to an elongation flow. The main objective of this simplified derivation is to illustrate the nature of dynamic tension. Thus the first assumption permits the description of the flow within the lamella in spherical coordinates. The second one imposes a diagonal form for the viscous stress tensor. The nonzeroth components of this tensor τ_{rr}, $\tau_{\theta\theta}$, and $\tau_{\varphi\varphi}$ are functions of the film thickness only. Therefore, the normal stress balances at both of the lamella interfaces are [28,24]

$$-\left(P_- + \frac{2\sigma_-}{R}\right) + \Pi_l(h_l) = -P_w + \tau_{rr}, \tag{28}$$

$$-\left(P_+ - \frac{2\sigma_+}{R}\right) + \Pi_l(h_l) = -P_w + \tau_{rr}. \tag{29}$$

As follows from Eqs. (28) and (29), the mean radius R of the lamella can be calculated from the ordinary Laplace equation in the same manner as in equilibrium thermodynamics. The lamella tension and the pressure difference in the Laplace equation should be treated as dynamic values, because they differ from the equilibrium values by an amount lost due to the lamella motion. The Laplace equation gives the equation of motion for the individual lamella. If the radius R is expressed through the lamella chord radius $r_0 - \rho$, the apparent contact angle ψ is found from

$$\frac{\sin\psi}{(r_0-\rho)} = \frac{P_- - P_+}{2(\sigma_- + \sigma_+)}. \tag{30}$$

The same system of equations (28) and (29) provides the following relation between the lamella thickness, disjoining pressure, and normal stress:

$$\Pi_l(h_l) = \tfrac{1}{2}(P_- + P_+ - 2P_w(\xi)) + \tau_{rr}. \tag{31}$$

At this step, the rheological model for the lamella is required. It should be noted, however, that there is no conventional rheological model for foam lamellae because the structure of the foam films remains enigmatic. The following possible structures have been suggested: a smecticlike structure [40,41], a cubic lattice of ordered micelles [42], a fluid with a specific exponential correlation function [43], a bilayer of surfactants with aqueous core [44], and a gel-like structure [45]. Each of them requires an individual approach to the rheology. Specific surface properties of the foam films also dictate an additional modification of the rheological relations [46]. Therefore, it is difficult to designate specifically the form of the normal stress. Nevertheless, quite a lot of rheological laws permit the expression of the normal stress τ_{rr} in terms of the extensional strains rates $e_{rr} = d\ \ln(h_l)/dt$ and $e_{\varphi\varphi} = d\ \ln(r_0-\rho)/dt$ [47]. The normal stress τ_{rr} can be expressed then through the time derivative of the lamella thickness and chord radius. For instance, assuming that the lamella is deformed as a Newtonian fluid, we have the following linear relation between the respective component of the stress tensor and the extensional strain rate: $\tau_{rr} = \mu_l d\ \ln h_l/dt$, where μ_l is the lamella viscosity. Thus the lamella thickness depends implicitly upon the dynamic pressure drop, the magnitude of the pressure within the lamella, and the height of the crest. Since the pressure within the lamella must be equal to the pressure in the wetting fluid, Eq. (31) provides a relation between the parameters of the wetting film and the lamella thickness. If the functional form of the disjoining pressure is given beforehand, the lamella thickness can be found from Eq. (31) at any instant of time as a function of the input parameters. Finally, the dynamic tension of the lamella can be found from the balance of tangential forces as

$$2\gamma_d = \sigma_- + \sigma_+ + \int_{h_l}^{\infty} \Pi_l(h)dh - h_l(P_w(\xi) - P_+) + h_l\tau_{\theta\theta}. \tag{32}$$

Here we use $h_l P_+$ as a reference or background tension. Substituting the difference $(P_w(\xi) - P_+)$ from Eq. (29) into Eq. (32), we arrive at the formula for dynamic tension

$$2\gamma_d = 2\gamma + \Delta_- + \Delta_+ - h_l(\tau_{\theta\theta} - \tau_{rr}), \tag{33}$$

where $\Delta_i = \sigma_i - \sigma$.

The above analysis demonstrates how the lamella rheology influences its dynamic tension. Thus, for a Newtonian fluid, the θ component of the stress tensor is a linear function of the respective component of the extensional strain rate $e_{\theta\theta}$. Because of the fluid incompressibility, one has $e_{\theta\theta} = -e_{rr} - e_{\varphi\varphi}$. Therefore, $\tau_{\theta\theta}$ can be expressed through the film thickness and the lamella radius. In conclusion of this subsection, it should be emphasized that all the lamella parameters, such as its thickness, apparent contact angle and tension, are self-consistently connected with the wetting film parameters.

(d) Pressure continuity. The lubrication approximation implies that the pressure in the wetting fluid at the contact line varies continuously, i.e., the equation $P_w|_{x=\xi-0} = P_w|_{x=\xi+0}$ holds. Making use of Eq. (20), the desired boundary condition is written as

$$P_- - \sigma_- 2H|_{x=\xi-0} = P_+ - \sigma_+ 2H|_{x=\xi+0}. \tag{34}$$

(e) Mass balance. The final two boundary conditions are given by the mass balances in the whole system lamella plus wetting film, and in the microelement of the moving boundary. The former one depends on the mass exchange at the ends of the capillary. For the latter one, consider the following analysis of infinitesimal mass variation. The lamella passes the distance $d\xi$ during the time interval dt. The mass change is $(\rho - \min(h_-|_{x\to-\infty}; h_+|_{x\to\infty}))d\xi$; on the other hand, this change is the flow influx qdt. Therefore,

$$(\rho - \min(h_-|_{x\to-\infty}; h_+|_{x\to\infty}))\frac{d\xi}{dt} = q|_{x\to\xi},$$
$$q|_{x=\xi-0} = q|_{x=\xi+0}. \tag{35}$$

A similar procedure can be used for a derivation of the boundary condition at the moving contact line even if the lamella squeezes a portion of liquid into the Plateau border. The only modification concerns the integral mass balance; that is, we must either account for the fact that the total

liquid volume in the system ''lamella plus wetting film'' remains the same, or presume some law for fluid depletion. If we assume that the total mass is conserved, the following additional constraint to the admissible crest height holds:

$$(h_l\Sigma-\pi(r_0-\rho_0)^2h_{l_0})$$
$$=\pi\int_{-\infty}^{\infty}[r_0^2-(r_0-h_\pm(x))^2]-[r_0^2-(r_0-h_0(x))^2]dx, \tag{36}$$

where h_{l_0} is the equilibrium thickness of the lamella, $h_0(x)$ is the integral of Eq. (2), ρ_0 is the height of the equilibrium crest, and Σ denotes the area of moving lamella.

Thus, the free boundary problem is formulated in terms of the wetting film thickness. Equations (19)–(36) must be combined with the boundary conditions at the ends of the wetting films. At the end where the film remains at rest, the film thickness has the well defined value $h_+(\infty,t)=h_\infty$. At the same time, the thickness of the residual film h_-^∞ at the opposite end is unknown in advance, and has to be found. It seems reasonable to assume that all the spatial derivatives at both ends vanish, i.e., the wetting films tend to be flat at the ends. Finalizing the statement, it should be noted that the initial conditions depend on the scenario of loading.

IV. TRAVELING WAVE SOLUTION

To demonstrate the characteristic features of the model developed in Sec. III, we analyze the traveling wave solution of the form

$$h_\pm(x,t)=h_\pm(s),\quad s=x-Ut,$$

where U is the velocity of the lamella propagation over the wetting film. This solution describes a steady motion of an individual lamella over the prewetted pore, as well as a steady motion of the ith lamella of a moving bubble train. Since the lamella moves steadily, the viscous stresses disappear, $\tau_{\theta\theta}=\tau_{rr}=\tau_{\varphi\varphi}=0$, provided that the lamella behaves like an ordinary liquid film. If the lamella is a liquid crystal, the additional stresses should be specified. We restrict ourselves to the analysis of a fluidlike lamella, so that the dynamic tension $2\gamma_d$ and the lamella disjoining pressure $\Pi_l(h_l)$ are influenced by the viscous forces only implicitly.

The integration of the governing equations with respect to s leads to the equation

$$-U(h_\pm-h_\pm^\infty)=\frac{h_\pm^3}{3\mu}\frac{dP_w}{ds}, \tag{37}$$

in which the minus sign is associated with the left infinity, and the plus sign denotes the thickness of the advancing meniscus; index ''∞'' denotes the value of the respective quantity at infinity. The integration of Eq. (37) results into the following relation between the pressure drop and the lamella speed:

$$-3\mu U\left(\int_0^{+\infty}\frac{h_+-h_+^\infty}{h^3}\,ds+\int_{-\infty}^{0}\frac{h_--h_-^\infty}{h^3}\,ds\right)=P_+-P_-. \tag{38}$$

The mass balance [Eq. (35)] reveals that the residual film thickness and the film thickness at the right infinity are the same, i.e.,

$$h_-^\infty=h_+^\infty=h_\infty. \tag{39}$$

Hence the lamella moves steadily only by virtue of the presence of the pressure difference in the liquid within uniform pieces of the lining film. This result justifies the hypothesis of Hirasaki and Lawson [5].

A. Classification of displacement regimes

Although the general analysis of the similarity solution allows one to obtain a number of useful relations [Eqs. (37)–(39)], it is still quite complicated and requires the application of numerical methods. More tractable analytical results can be obtained if we specialize the range of the input physical parameters. Furthermore, introducing the pair $\cos\beta_\pm(h)$ in the same way as that is defined in Eq. (8), and rewriting Eq. (37) as

$$3\epsilon\,\mathrm{Ca}\,\frac{(h-h_\infty)\cos\beta_\pm(h)}{h^3\sqrt{1-\cos\beta_\pm^2(h)}}=-\frac{d^2\cos\beta_\pm(h)}{dh^2}+\frac{1}{\sigma}\frac{d\Pi}{dh}, \tag{40}$$

one can classify the solutions with respect to the range of variation of the capillary number Ca. Note that we choose the angles in Eqs. (40) by using their definition at the point $h=\rho$ (Fig. 3). Moreover, the change of variables can be applied only if the functions $\cos\beta_\pm(h)$ vary monotonically. Hence, parameter ϵ is positive for a receding meniscus, $\epsilon=+1$, and it is negative ($\epsilon=-1$) if the profile of the advancing meniscus is described by a monotonically decreasing function [see Fig. 4(a), top]. However, if the meniscus possesses an indentation [Fig. 4(a), bottom], the profile of the advancing meniscus must be described by two functions β_+^d and β_+^i; the first one is a decreasing function and the other one is an increasing function. In other words, the stepwise function $\epsilon(h)$ can be introduced as follows: $\epsilon(h)=-1$ if $h^*\leqslant h\leqslant\rho$, and $\epsilon(h)=+1$ if $h^*\leqslant h\leqslant h_\infty$, provided that the critical thickness h^* must be found by matching both branches of the solution. Thus one cannot specify in advance the form of the stepwise function $\epsilon(h)$, and an additional analysis should be done in order to select a suitable shape of the Plateau border. Mathematically, this means that it is necessary to clarify a behavior of the functions $\cos\beta_\pm(h)$ at the ends of capillary $h=h_\infty$.

Due to the boundary conditions, the asymptotic behavior of the solution can be described by the following general form: $\cos\beta_\pm(h)\approx 1-A_\pm(h-h_\infty)^k$. Substituting this anzatz into Eq. (40), one obtains $k\geqslant 2$, so that the linear term is absent. Parameters $A_\pm$ can be found from the equations

$$\mp\frac{3\,\mathrm{Ca}}{\Lambda^{3/2}}=u_\pm(u_\pm^2-1),\quad \Lambda>0, \tag{41}$$

$$\mp\frac{3\,\mathrm{Ca}}{(-\Lambda)^{3/2}}=u_\pm(u_\pm^2+1),\quad \Lambda<0, \tag{42}$$

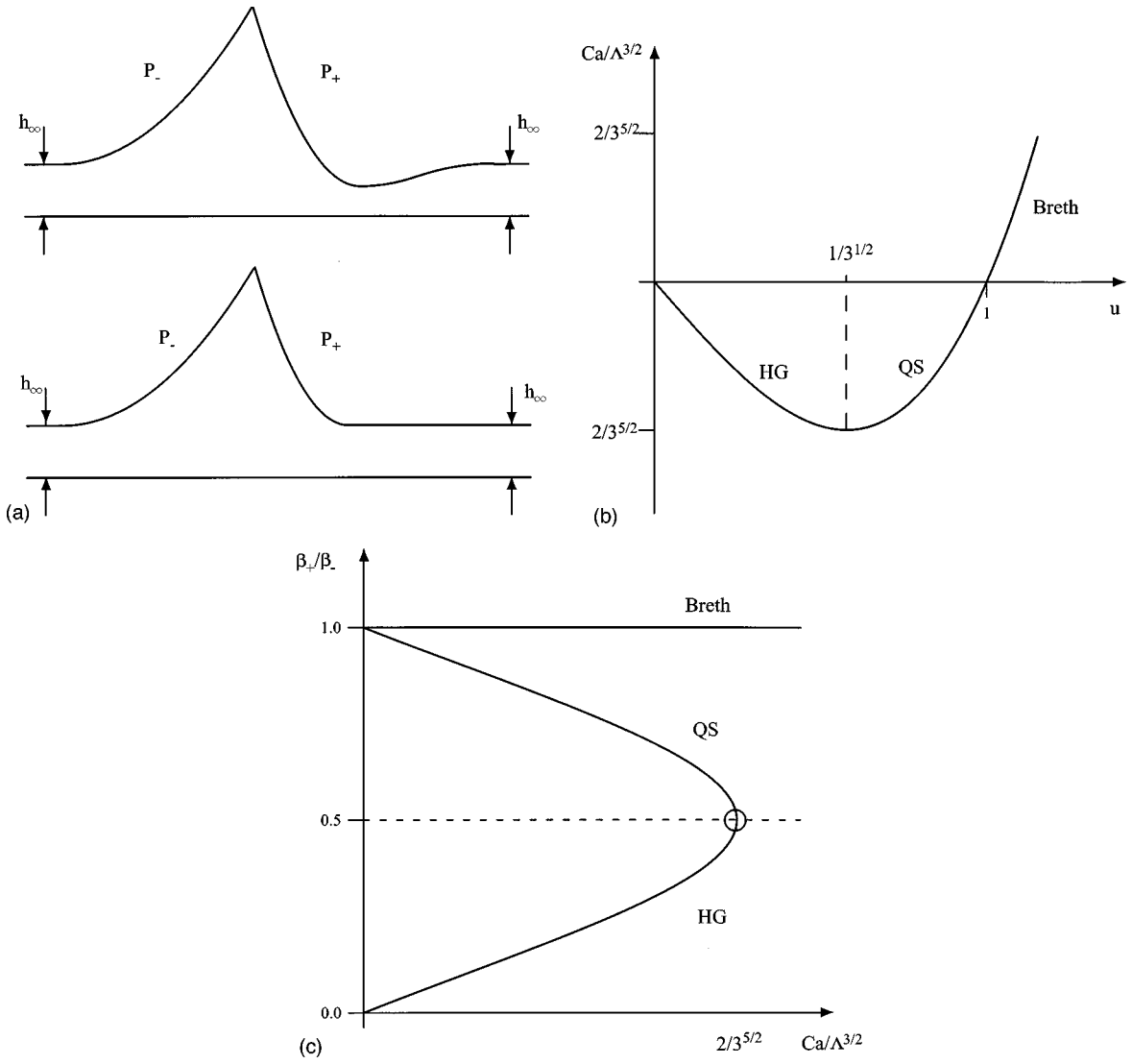

FIG. 4. (a) The presence of an indentation in the advancing meniscus (at the bottom) allows one to select the specific regimes of lamella sliding. (b) Graphic solution of the cubic equation (42). QS, HG, and Breth denote quasistatic, Hervet–de Gennes, and Bretherton regimes, respectively. (c) The ratios between advancing and receding inclination angles vs parameter $\mathrm{Ca}/\Lambda^{3/2}$ for different regimes of lamella sliding.

where $u_{\pm}=h_{\infty}\sqrt{2A_{\pm}}/\sqrt{|\Lambda|}$, and $\Lambda=(-h_{\infty}^2/\sigma)d\Pi/dh(h_{\infty})$. Parameter Λ can be treated as the stability parameter. If it is negative, the film is thermodynamically unstable and breaks down into droplets. Otherwise, the wetting film exists [16,39].

The analysis of the cubic polynomial equations (41) and (42) reveals distinguishing regimes in the behavior of the wetting film during the lamella motion. Only positive roots are physically acceptable. One can see that there is a unique solution u_{-} associated with the plus sign on the left hand sides of Eqs. (41) and (42). However, if the right interface tends to its flat state from below, i.e., if the thickness increases at infinity, then, for the ''plus'' cosine, the plus sign must be taken in the left hand side of Eqs. (41) and (42). Thus the disappearance of the roots, which is associated with the minus sign in the left hand side of Eqs. (42), can be attributed to the presence of an indentation in the wetting film ahead of the lamella.

Hence the regimes of lamella sliding can be classified according to the characteristic behavior of the inclination angles $\beta_{\pm}(h)$ at plus and minus infinity, provided that the approximate equality $\beta_{\pm}\approx\sqrt{2A_{\pm}}(h-h_{\infty})$ holds. The peculiarities in the behavior of the roots of the cubic equation classify the regimes. Explicitly, the growth rate of advancing angle $\beta_{+}/(h-h_{\infty})\approx\sqrt{2A_{+}}$ is a convenient quantity to distinguish the regimes. Below we consider only a ''regular'' case of lamella displacement, when no indentation of the receding meniscus occurs.

Negative stability parameter. The inclination angles behave identically,

$$\frac{\beta_{\pm}^{\mathrm{HG}}}{(h-h_{\infty})}\approx\frac{2}{h_{\infty}}\sqrt{|\Lambda|/3}\,\sinh\left(\frac{1}{3}\,\mathrm{arcsinh}\,\frac{3^{5/2}}{2}\,\mathrm{Ca}/|\Lambda|^{3/2}\right),$$

but the advancing meniscus forms an indentation. In the characteristic limit $\mathrm{Ca}/|\Lambda|^{3/2}\to 0$, the linear term on the right hand side of Eq. (42) dominates the quibic one. In other words, similarly to the Hervet–de Gennes (HG) regime of

wetting [48], the viscous and surface forces govern the flow pattern. Hence, the regime is called the Hervet–de Gennes regime.

Positive stability parameter. There are at least three possible regimes of lamella sliding: the Bretherton regime, the Hervet–de Gennes regime, and a quasistatic regime of motion. Figure 4(b) shows a scheme for selection of the respective roots.

(i) Bretherton regime. Both advancing and receding inclination angles behave identically,

$$\frac{\beta_{\pm}^{\mathrm{Breth}}}{(h-h_{\infty})} \approx -\frac{2}{h_{\infty}}\sqrt{\Lambda/3}\,\cos\left(\frac{1}{3}\arccos\left(-\frac{3^{5/2}}{2}\,\mathrm{Ca}/\Lambda^{3/2}\right)+2\pi/3\right), \tag{43}$$

but a distinguishing indentation at the advancing meniscus occurs. In the limiting case $\mathrm{Ca}/\Lambda^{3/2}\to 0$, the capillary and viscous forces dominate the surface forces. Since Bretherton [4] was the first to consider a similar problem of bubble displacement, this case is called the Bretherton regime of lamella displacement. Both the Hervet–de Gennes and quasistatic regimes may be realized only in the range $0 \leqslant \mathrm{Ca}/\Lambda^{3/2} \leqslant 2/3^{5/2}$.

(ii) Hervet–de Gennes regime. The growth rates of advancing and receding angles have the forms

$$\frac{\beta_{+}^{\mathrm{HG}}}{(h-h_{\infty})} = \frac{2}{h_{\infty}}\sqrt{\Lambda/3}\,\cos\left(\frac{1}{3}\arccos\left(-\frac{3^{5/2}}{2}\,\mathrm{Ca}/\Lambda^{3/2}\right)+4\pi/3\right),$$

$$\frac{\beta_{-}^{\mathrm{HG}}}{(h-h_{\infty})} = -\frac{2}{h_{\infty}}\sqrt{\Lambda/3}\,\cos\left(\frac{1}{3}\arccos\left(-\frac{3^{5/2}}{2}\,\mathrm{Ca}/\Lambda^{3/2}\right)+2\pi/3\right).$$

If parameter $\mathrm{Ca}/\Lambda^{3/2}$ is small, the surface and viscous forces dominate the capillary forces, so that the growth rate of the advancing inclination angle can be estimated as $\beta_{+}^{\mathrm{HG}}/(h-h_{\infty}) \approx 3\,\mathrm{Ca}/\Lambda h_{\infty}$. At the same time, the rear meniscus tends to keep its equilibrium shape. Consequently, the growth rate of the receding angle can be approximated as $\beta_{-}^{\mathrm{HG}}/(h-h_{\infty}) \approx \Lambda^{1/2}/h_{\infty}$, and there is a difference in advancing and receding angles. Figure 4(c) shows that the ratio of the respective growth rates may be perceptible if parameter $\mathrm{Ca}/\Lambda^{3/2}$ tends to its critical value $2/3^{5/2}$.

(iii) Quasistatic regime. In a quasistatic (QS) regime of lamella sliding, the growth rates are expressed as

$$\frac{\beta_{+}^{\mathrm{QS}}}{(h-h_{\infty})} = \frac{2}{h_{\infty}}\sqrt{\Lambda/3}\,\cos\left(\frac{1}{3}\arccos\left(-\frac{3^{5/3}}{2}\,\mathrm{Ca}/\Lambda^{3/2}\right)\right),$$

$$\frac{\beta_{-}^{\mathrm{QS}}}{(h-h_{\infty})} = -\frac{2}{h_{\infty}}\sqrt{\Lambda/3}\,\cos\left(\frac{1}{3}\arccos\left(-\frac{3^{5/2}}{2}\,\mathrm{Ca}/\Lambda^{3/2}\right)+2\pi/3\right).$$

For $\mathrm{Ca}/\Lambda^{3/2} \ll 1$, the capillary and surface forces play a dominant role. A remarkable difference compared to the Hervet–de Gennes regime concerns the growth rates of the advancing and receding angles that are identical to that of the Bretherton regime, $\beta_{+}^{\mathrm{QS}}/\beta_{-}^{\mathrm{QS}} \approx 1$. However, an indentation at the advancing meniscus is absent. As parameter $\mathrm{Ca}/\Lambda^{3/2}$ approaches $2/3^{5/2}$, the ratio $\beta_{+}^{\mathrm{QS}}/\beta_{-}^{\mathrm{QS}}$ decreases up to $\frac{1}{2}$. At this point, the difference in the Hervet–de Gennes and quasistatic regimes disappears. If parameter $\mathrm{Ca}/\Lambda^{3/2}$ further increases, we inevitably achieve the Bretherton regime with $\beta_{\pm}^{\mathrm{Breth}}$ given by Eq. (43).

Although the above classification seems to be clear, the selection principle for the Hervet–de Gennes and quasistatic regimes remains enigmatic. In this paper we concentrate solely on the analysis of the quasistatic regime of lamella motion.

B. Quasistatic motion

At low speeds, the displacement can be classified as quasistatic. In this regime, the film profile is governed almost entirely by the capillary and disjoining pressures. In other words, one expects that the viscous term in Eq. (40) only slightly alters the basic shape of the equilibrium Plateau border. Therefore, the solution of Eq. (40) can be represented as an asymptotic expansion in terms of the small capillary number Ca. It should be stressed here that the presence of the disjoining pressure allows one to seek the *regular asymptotic solution*, which is in contrast to the Bretherton *singular asymptotic solution* [4,49]. In the Bretherton solution, the singularity with respect to Ca originates from a specific matching of the spherical caps of equilibrium menisci with a uniform film. The classical formulation suggests the only possibility for the equilibrium coexistence of menisci and walls, namely, only contact with a dry wall is allowed. Consequently, any theory that neglects the surface forces encounters a problem in matching; one has to link a moving film with menisci whose spherical caps at the wall form a finite contact angle. Thus to smooth out the angle that the equilibrium meniscus forms with the wetting uniform film, the theory should invoke a singular perturbation technique. In the presence of equilibrium wetting film, one may use the ordinary perturbation theory, because the shape of the moving Plateau border is compatible with its basic equilibrium profile.

We seek the asymptotic solution in the form $\cos\beta_{\pm}(h)=\cos\beta(h)+\mathrm{Ca}\,\nu_{\pm}$. In order to guarantee that the second term is smaller than the first one, the following applicability condition is prescribed

$$\mathrm{Ca}\lesssim\left(-\frac{h_{\infty}^{2}}{\sigma}\frac{d\Pi}{dh}\right)^{3/2}\ll 1. \tag{44}$$

The principal term $\cos\beta(h)$ was found in Sec. II. For the first term proportional to the capillary number, we have the following equations:

$$\mp 3\frac{(h-h_{\infty})\cos\beta(h)}{h^{3}\sqrt{1-\cos^{2}\beta(h)}}=-\frac{d^{2}\nu_{\pm}}{dh^{2}}. \tag{45}$$

Taking into account the behavior of the solution at the point $h=h_{\infty}$, the solution to Eqs. (45) can be written as

$$\nu_{\pm}=\pm 3\int_{h_{\infty}}^{h}\frac{(h-t)(t-h_{\infty})\cos\beta(t)}{t^{3}\sqrt{(1-\cos^{2}\beta(t))}}\,dt. \tag{46}$$

Using this solution, one can express all the physical parameters. In particular, accounting for Eq. (34), the relation between the applied pressure drop and the lamella speed takes the form of the Newtonian friction law

$$\Delta P=P_{-}-P_{+}=6\mu U\int_{h_{\infty}}^{\rho_{0}}\frac{(t-h_{\infty})\cos\beta(t)}{t^{3}\sqrt{(1-\cos^{2}\beta(t))}}\,dt. \tag{47}$$

The angle between the hemispherical lamella and the chord also depends linearly on the lamella speed; the following formula holds:

$$\psi=\frac{3(r_{0}-\rho_{0})\mu U}{2\sigma}\int_{h_{\infty}}^{\rho_{0}}\frac{(t-h_{\infty})\cos\beta(t)}{t^{3}\sqrt{(1-\cos^{2}\beta(t))}}\,dt. \tag{48}$$

Therewith, the balance of forces at the contact line, Eqs. (26) and (27), requires one to make the correction to the contact angles in the form $\beta_{\pm}(\rho)=\beta_{0}+\beta_{\pm}^{1}$, where

$$\beta_{\mp}^{1}=\pm\left(\frac{F_{\mathrm{fr}}}{2\gamma}-\psi\right).$$

Since the angles differ only in sign, the boundary conditions (24)–(25) serve as the solvability condition. From the latter, the friction force is found as

$$F_{\mathrm{fr}}=6\mu U\int_{h_{\infty}}^{\rho_{0}}\left(\frac{\gamma(r_{0}-\rho_{0})}{2\sigma}-(\rho_{0}-t)\right)\times\frac{(t-h_{\infty})\cos\beta(t)}{t^{3}\sqrt{(1-\cos^{2}\beta(t))}}\,dt. \tag{49}$$

The reminder of unused boundary conditions reveals that the lamella maintains its thickness unchanged during the stretching. In other words, the deviation of the lamella thickness relative to the equilibrium thickness is at least one order smaller. The lamella tension is also maintained at its equilibrium level, and the height of the Plateau border crest remains the same. Hence the first order approximation allows the vertex to rotate, but the radius of lamella rim keeps its equilibrium value. It can be checked by the direct substitution of the solution into Eq. (36) that the wetting film does not lose its mass, and no extra mass comes from the lamella.

Thus, during its slow creep, the lamella slightly bulges to form a hemispherical sail, with the radius being inversely proportional to the lamella velocity [Eqs. (30) and (48)]. The physical parameters of the contact line—the lamella tension, the rim radius, and the lamella thickness—altogether retain their equilibrium values.

V. DISCUSSION AND CONCLUSIONS

The results presented in this paper point directly to the critical question of how the substrate wettability influences the lamella friction. In our theory, the wettability conditions are expressed through specific disjoining pressure isotherms. Because of a rather wide spectrum of admissible disjoining pressure isotherms, one can imagine a variety of displacement regimes, depending on the wetting film thickness. Among the family of isotherms, specific foaming agents somehow select acceptable isotherms, so that the frothing solutions can be classified relatively to their wettability of the given substrate [38,50]. The foaming agents are made of a mixture of several surfactants, and the mother liquid used is not pure. Therefore, the real situation is quite complicated. Usable literature results are sparse, and they collect disjoining pressure isotherms for either free or wetting films. A usual model foaming system is a water solution of sodium dodecyl sulfate (SDS) with a sodium chloride additive, whose wettability with respect to quartz and foaminess are well documented [27,36,41]. Since SDS is an anionic surfactant, the behavior of the corresponding foam films is determined by the competition between the attractive van der Waals forces and the repulsive screened Coulomb forces due to the dissociation of ions from the amphiphilic molecules [16,51]. Churaev and Zorin [36] showed that for film thicknesses of about 100 nm and surfactant concentrations below the critical micelle concentration, electrostatic interactions dominate. Therefore, the disjoining pressure isotherm can be approximated by the Derjaguin-Landau formula $\Pi=A_{\mathrm{DL}}/h^{2}$, with $A_{\mathrm{DL}}\approx 10^{-12}-10^{-11}\ \mathrm{J\,m^{-2}}$. Taking into account that the presented theory may be applied if and only if inequality (44) holds, one can reformulate the validity condition for the theory as

$$\mathrm{Ca}\lesssim\left(\frac{2A_{\mathrm{DL}}}{\sigma h_{\infty}}\right)^{3/2}\ll 1.$$

In this range of capillary numbers, the leading order term of asymptotic expansion with respect to $\alpha_{2}=A_{\mathrm{DL}}/\sigma h_{\infty}$ can be calculated as (see the Appendix)

$$\Delta P\approx\mathrm{Ca}\,\frac{(2\sigma)^{3/2}}{A_{\mathrm{DL}}^{1/2}}\frac{1}{h_{\infty}^{1/2}}.$$

For example, if the film thickness is of the order of 100 nm, and if the surface tension is of the order of 30 mN/m, the pressure drop is $\mathrm{Ca}\times 10^{7}$ Pa. On the other hand, the range of admissible capillary numbers lies within the interval $\mathrm{Ca}\lesssim 10^{-5}-10^{-4}$. Therefore, if $\mathrm{Ca}\approx 10^{-4}$, the applied pressure

drop must be of the order of 10^3 Pa, that is a value near the capillary pressure, under which a single lamella created from a dilute solution breaks [27]. Hence one may expect that the lamella most likely disappears before it reaches a stationary regime of motion.

If the dispersion forces are responsible for the film stability, a similar calculation can be performed for the van der Waals isotherms of disjoining pressure, $\Pi = A_{\mathrm{vdW}}/h^3$. In the leading order approximation with respect to the parameter $\alpha_3 = A_{\mathrm{vdW}}/\sigma h_\infty^2$, the applied pressure drop can be expressed as (see the Appendix)

$$\Delta P \approx 6(3^{1/2} - \ln(2+3^{1/2}))\mathrm{Ca}\,\frac{\sigma^{3/2}}{A_{\mathrm{vdW}}^{1/2}}.$$

Although the pressure drop does not depend on the film thickness explicitly, the connection can be established by means of Eq. (44). Thus

$$\mathrm{Ca} \lesssim \left(\frac{3A_{\mathrm{vdW}}}{\sigma h_\infty^2}\right)^{3/2} \ll 1.$$

The estimations [51] $A_{\mathrm{vdW}} \approx 10^{-21} - 10^{-19}$ J, $\sigma \approx 30$ mN/m, and $h_\infty \approx 50$ nm lead to the following admissible range of capillary numbers: $\mathrm{Ca} \lesssim 10^{-6} - 10^{-3}$. Within this range, the pressure drop can be estimated as $\Delta P \approx 10^3 - 10^6$ Pa. There is a speed interval, for which the lamella most likely disappears.

A moving lamella is very sensitive to environmental conditions; the fact that the lamella is thermodynamically stable at rest does not imply its stability in motion. The experimental observation of the effect of dynamic coarsening of foams in porous media was reported by Khatib, Hirasaki, and Falls [52]. However, no explanation of this phenomenon was proposed in the literature [1,2]. Our analysis suggests that the dynamic coarsening effect is caused by anomalous friction of each individual lamella under, from the thermodynamic point of view, critical conditions. If the hydrodynamic conditions are limited to the quasistatic region, the principal factors that affect the apparent viscosity of lamellae in uniform capillaries are thermodynamic ones. Viscous, capillary, and surface forces altogether modify the Plateau border interfaces that are deformed against the restoring force of the surface and lamella tensions. However, if condition (44) is satisfied, the friction force is determined solely by the shape of equilibrium menisci. Since the Plateau border spreads over rather a large distance (see Sec. II), the resulting viscous dissipation is anomalous.

Three limiting regimes of the lamella friction are found. Only for one of them is the friction proportional to the lamella velocity; for two others, the friction is non-Newtonian (Hervet–de Gennes and Bretherton models). The Bretherton regime selects a unique film. The lamella can propagate steadily if and only if the thickness has a certain value. Furthermore, there are no other traveling wave solutions [15].

For the problem of a bubble displacement [14,30], the increasing of the displacement speed reduces the apparent contact angle between the substrate and bubble interface until the angle eventually reaches zero. As a result, a visually detectable film is deposited independently of the surface wettability. One may expect that a similar change of the motion regimes occurs for a foam lamella. However, the mechanism of transition between the quasistatic, Hervet–de Gennes, and Bretherton regimes still remains an open question. A detailed experimental analysis of foam motion in smooth capillaries at low capillary numbers could clarify the situation.

ACKNOWLEDGMENTS

We are grateful to P. Yakubenko for assistance in improving the text. K.K. thanks the Department of Hydraulic Engineering, The Royal Institute of Technology (Stockholm) for their hospitality. This work was supported by The Royal Swedish Academy of Sciences (Project No. 1264).

APPENDIX

In practice, the customary approximation of a disjoining pressure isotherm is $\Pi(h) = A_n/h^n$. Here we present some useful formulas obtained for any disjoining pressure isotherm of such a form with an integer $n \geqslant 2$. In particular, Eq. (17) becomes

$$\cos\,\beta(h) = -\frac{\alpha_n}{n-1}\left(\frac{(h/h_\infty)^n(n-1) - n(h/h_\infty)^{n-1} + 1}{(h/h_\infty)^{n-1}}\right) + 1, \tag{A1}$$

where $\alpha_n = A_n/\sigma h_\infty^{n-1}$. Using boundary condition (11), α_n can be expressed in terms of the crest height and inclination angle:

$$\alpha_n = \frac{(1-\cos\,\beta_0)(n-1)}{(\rho_0/h_\infty)(n-1) - n + (\rho_0/h_\infty)^{1-n}}. \tag{A2}$$

Substituting Eq. (A1) into Eq. (18), one can obtain

$$x(t) = \left(\frac{n-1}{\alpha_n}\right)^{1/2}\int_{\rho_0}^{t}\frac{g(h)}{(h/h_\infty - 1)}\,dh$$

$$= \left(\frac{n-1}{\alpha_n}\right)^{1/2} h_\infty(g(t)\ln(t-h_\infty) - g(\rho_0)\ln(-h_\infty+\rho_0)) - \left(\frac{n-1}{\alpha_n}\right)^{1/2}\int_{\rho_0}^{t} g'(h)\ln(-h_\infty+h)h_\infty dh,$$

where

$$g(h)=\frac{-\frac{\alpha_n}{n-1}\left((h/h_\infty)^n(n-1)-n(h/h_\infty)^{n-1}+1\right)+(h/h_\infty)^{n-1}}{\left[\left(2(h/h_\infty)^{n-1}-\frac{\alpha_n}{n-1}\left((h/h_\infty)^n(n-1)-n(h/h_\infty)^{n-1}+1\right)\right)\sum_{l=0}^{n-2}(l+1)(h/h_\infty)^l\right]^{1/2}}.$$

For $h\to h_\infty$, one has $x(h)\simeq\sqrt{\rho_0 h_\infty/(1-\cos\beta_0)n}\,\ln(h/h_\infty-1)$. Hence, the size of the transition region can be estimated as $l_{\rm pl}\sim\sqrt{\rho_0 h_\infty/(1-\cos\beta_0)n}$.

For small α_n, in the leading order the Plateau border [Eq. (18)] can be approximated as

$$x(t)\simeq\left(\frac{n-1}{2\alpha_n}\right)^{1/2}\int_{\rho_0}^{t}\frac{1}{(h/h_\infty-1)}\frac{(h/h_\infty)^{(n-1)/2}}{\left(\sum_{l=0}^{n-2}(l+1)(h/h_\infty)^l\right)^{1/2}}\,dh. \tag{A3}$$

Similarly, in leading order with respect to α_n, the first correction in the asymptotic solution for the inclination angles [Eq. (46)] is

$$\nu_{\pm}\simeq\pm 3\left(\frac{n-1}{2\alpha_n}\right)^{1/2}\int_{h_\infty}^{h}\frac{(h-t)(t/h_\infty-1)(t/h_\infty)^{(n-7)/2}}{h_\infty^2\sqrt{(t/h_\infty)^n(n-1)-n(t/h_\infty)^{n-1}+1}}\,dt. \tag{A4}$$

The relation between the applied pressure drop and the lamella speed [Eq. (47)] can be represented as

$$\Delta P\simeq 6\,\mathrm{Ca}\,\sigma\left(\frac{n-1}{2\alpha_n}\right)^{1/2}\int_{h_\infty}^{\infty}\frac{(t/h_\infty-1)(t/h_\infty)^{(n-7)/2}}{h_\infty^2\sqrt{(t/h_\infty)^n(n-1)-n(t/h_\infty)^{n-1}+1}}\,dt, \tag{A5}$$

and Eq. (49) is rewritten as

$$F_{\rm fr}=3\,\mathrm{Ca}\,\sigma\left(\frac{n-1}{2\sigma_n}\right)^{1/2}\frac{\gamma r_0}{\sigma}\int_{h_\infty}^{\infty}\frac{(t/h_\infty-1)(t/h_\infty)^{(n-7)/2}}{h_\infty^2\sqrt{(t/h_\infty)^n(n-1)-n(t/h_\infty)^{n-1}+1}}\,dt. \tag{A6}$$

Consider two physically justified examples of the disjoining pressure isotherm of the type under consideration. If the electrostatic interactions dominate others, and, moreover, the Derjaguin-Landau approximation is responsible for the disjoining pressure, one has $n=2$ and $A_2=A_{\rm DL}$. Equation (18), that describes the profile of the Plateau border, can be explicitly integrated to give

$$x=-\left(\frac{2}{\alpha_2}\rho_0 h_\infty-(\rho_0-h_\infty)^2\right)^{1/2}+\left(\frac{2}{\alpha_2}hh_\infty-(h-h_\infty)^2\right)^{1/2}$$
$$+\frac{h_\infty}{\sqrt{2\alpha_2}}\ln\frac{h-h_\infty}{\rho_0-h_\infty}-\frac{h_\infty}{\sqrt{2\alpha_2}}\ln\frac{\sqrt{2}\sqrt{2hh_\infty-\alpha_2(h-h_\infty)^2}+h_\infty+h}{\sqrt{2}\sqrt{2\rho_0 h_\infty-\alpha_2(\rho_0-h_\infty)^2}+h_\infty+\rho_0},$$

where $\alpha_2=A_{\rm DL}/\sigma h_\infty$. Using Eq. (A2) with $n=2$, equation for profile of the Plateau border can be rewritten in terms of the measurable parameters ρ_0, h_∞, and β_0. If $\cos\beta_0=1$, the solution is identical to the solution found by Neimark and Kheifetz [32] for profile of the meniscus in a slot. In the general case $\cos\beta_0\neq 1$, the first correction proportional to the capillary number [Eq. (46)] becomes

$$\nu_+=-\nu_-=\frac{3}{2}\frac{\alpha_2(h+h_\infty)-h}{\alpha_2^2 hh_\infty}\sqrt{2\alpha_2 hh_\infty-\alpha_2^2(h-h_\infty)^2}-\frac{3}{\sqrt{2\alpha_2}}\left(2-\frac{h}{h_\infty\alpha_2}\right)$$
$$-3\left(\frac{1}{2}\frac{h/h_\infty}{\alpha_2^2}+1\right)\arcsin\frac{h+(h-h_\infty)\alpha_2}{h\sqrt{2\alpha_2+1}}+3\arcsin\frac{\alpha_2(h-h_\infty)-h_\infty}{h_\infty\sqrt{2\alpha_2+1}}+3\left(\frac{1}{2}\frac{h}{h_\infty\alpha_2^2}+2\right)\arcsin\frac{1}{\sqrt{2\alpha_2+1}}.$$

The relation between the applied pressure drop and the lamella speed takes the form

$$\Delta P=3\frac{\mathrm{Ca}\,\sigma}{h_\infty\alpha_2^2}\left(\frac{\alpha_2(\rho_0-h_\infty)-\rho_0}{\rho_0^2}\sqrt{2\alpha_2\rho_0 h_\infty-\alpha_2^2(\rho_0-h_\infty)^2}+\sqrt{2\alpha_2}\right)$$
$$-3\frac{\mathrm{Ca}\,\sigma}{h_\infty\alpha_2^2}\left(\arcsin\frac{\rho_0+\alpha_2(\rho_0-h_\infty)}{\rho_0\sqrt{2\alpha_2+1}}-\arcsin\frac{1}{\sqrt{2\alpha_2+1}}\right),$$

and the friction force is given by

$$F=\frac{6\ \mathrm{Ca}}{4\alpha_2^2 h_\infty}\,f,$$

where

$$f=[(\gamma(r_0-\rho_0)-2\rho_0\sigma)(\alpha_2(\rho_0-h_\infty)-\rho_0)-4\sigma\alpha_2\rho_0h_\infty]\times\frac{\sqrt{2\alpha_2\rho_0h_\infty-\alpha_2^2(\rho_0-h_\infty)^2}}{\rho_0^2}+\sqrt{2\alpha_2}(\gamma(r_0-\rho_0)-2\sigma(\rho_0-2h_\infty\alpha_2))$$

$$-(\gamma(r_0-\rho_0)-(2\rho_0+4\alpha_2^2h_\infty)\sigma)\arcsin\frac{\rho_0+\alpha_2(\rho_0-h_\infty)}{\rho_0\sqrt{2\alpha_2+1}}$$

$$+(\gamma(r_0-\rho_0)-2\sigma(\rho_0+4h_\infty\alpha_2^2))\arcsin\frac{1}{\sqrt{2\alpha_2+1}}-4\alpha_2^2h_\infty\sigma\ \arcsin\frac{\alpha_2(\rho_0-h_\infty)-h_\infty}{h_\infty\sqrt{2\alpha_2+1}}.$$

The second example concerns the films stabilized by the Lifshitz–van der Waals forces. If the dispersion forces dominate others, the isotherm of disjoining pressure has the form $\Pi=A_{\mathrm{vdW}}/h^3$. Though the problem cannot be integrated explicitly, asymptotic Eqs. (A3)–(A6) yield, respectively,

$$x\simeq\alpha_3^{-1/2}(\sqrt{2h+h_\infty}-\sqrt{2\rho_0+h_\infty})\left(\frac{\rho_0}{(1-\cos\beta_0)}\right)^{1/2}+\alpha_3^{-1/2}\left(\frac{\rho_0h_\infty}{(1-\cos\beta_0)}\right)^{1/2}\times\left(\frac{1}{\sqrt{3}}\ln\frac{h-h_\infty}{\rho_0-h_\infty}-2\ln\frac{\sqrt{2h+h_\infty}+\sqrt{3h_\infty}}{\sqrt{2\rho_0+h_\infty}+\sqrt{3h_\infty}}\right),$$

$$\nu_\pm\simeq\pm3\alpha_3^{-1/2}\left(\frac{\sqrt{3}h-\sqrt{(2h+h_\infty)h_\infty}}{h_\infty}+2\frac{(h+h_\infty)}{h_\infty}\ln\frac{\sqrt{h_\infty}+\sqrt{(2h+h_\infty)}}{(1+\sqrt{3})\sqrt{h}}\right),$$

$$\Delta P\simeq6\frac{\mathrm{Ca}\ \sigma}{h_\infty}\ \alpha_3^{-1/2}(\sqrt{3}-\ln(2+\sqrt{3})),$$

$$F_{\mathrm{fr}}=F_{\mathrm{fr}}=3\ \mathrm{Ca}\ \sigma\alpha_3^{-1/2}\frac{r_0}{h_\infty}\frac{\gamma}{\sigma}\ (\sqrt{3}-\ln(2+\sqrt{3})),$$

where $\alpha_3=A_{\mathrm{vdW}}/\sigma h_\infty^2$.

[1] A. R. Kovscek and C. J. Radke, in *Foams: Fundamentals and Applications in the Petroleum Industry*, edited by L. L. Schramm, Advances in Chemistry Series Vol. 242 (American Chemical Society, New York, 1994), pp. 115–164.

[2] W. R. Rossen, in *Foams: Fundamentals and Applications*, edited by R. K. Prud'homme and S. A. Khan (Dekker, New York, 1995), Vol. 57, pp. 413–464.

[3] R. Dautov, K. Kornev, and V. Mourzenko, Phys. Rev. E **56**, 6929 (1997).

[4] F. P. Bretherton, J. Fluid Mech. **10**, 166 (1961).

[5] G. J. Hirasaki and J. Lawson, Soc. Petr. Eng. J. **25**, 176 (1985).

[6] A. H. Falls, J. J. Musters, and J. Ratulowski, SPE Reservoir Eng. **4**, 55 (1989); J. Ratulowski and H. C. Chang, Phys. Fluids A **1**, 1642 (1989).

[7] K. G. Kornev and V. N. Kurdyumov, Zh. Eksp. Teor. Fiz. **106**, 457 (1994) [JETP **79**, 252 (1994)]; K. G. Kornev, *ibid.* **107**, 1895 (1995) [*ibid.* **80**, 1049 (1995)].

[8] M. P. Ida and M. J. Miksis, SIAM (Soc. Ind. Appl. Math.) J. Appl. Math. **55**, 23 (1995).

[9] L. W. Schwartz, H. M. Princen, and A. D. Kiss, J. Fluid Mech. **172**, 259 (1986).

[10] *Liquid Film Coating*, edited by F. Kistler and P. M. Schweizer (Chapman and Hall, London, 1997).

[11] E. Herbolzheimer (unpublished).

[12] H. C. Chang and J. Ratulowski (unpublished).

[13] J. D. Chen, J. Colloid Interface Sci. **109**, 34 (1986).

[14] G. F. Teletzke, Ph.D. thesis, University of Minnesota, 1983.

[15] J. Ratulowski and H. C. Chang, J. Fluid Mech. **210**, 303 (1990).

[16] B. V. Derjaguin, N. V. Churaev, and V. M. Muller, *Surface Forces* (Consultants Bureau, New York, 1987).

[17] B. Frank and S. Garoff, in *Dynamics in Small Confining Systems*, Symposium held November 28–December 1, 1994, Bos-

ton, MA, edited by J. M. Drake, J. Klafter, R. Kopelman, and S. M. Troian (Materials Research Society, Pittsburgh, 1995), pp. 39–51.
[18] E. M. Lifshitz and L. P. Pitaevskii, *Physical Kinetics* (Pergamon, Oxford, 1981).
[19] J. Stavans, Rep. Prog. Phys. **56**, 733 (1993); J. J. Bikerman, *Foams* (Springer-Verlag, New York, 1973).
[20] K. T. Chambers and C. J. Radke, in *Interfacial Phenomena in Petroleum Recovery*, edited by N. Morrow (Dekker, New York, 1990), p. 191.
[21] K. Kornev, A. Neimark, and A. Rozhkov (unpublished).
[22] J. Roof, Soc. Petr. Eng. J. **10**, 85 (1970); D. H. Everett and J. M. Haynes, J. Colloid Interface Sci. **38**, 125 (1972); L. I. Kheifets and A. V. Neimark, *Multiphase Processes in Porous Media* (Khimia, Moscow, 1982).
[23] K. K. Mohanty, Ph.D. thesis, University of Minnesota, 1981.
[24] I. B. Ivanov and P. A. Kralchevsky, in *Thin Liquid Films: Fundamentals and Applications*, edited by I. B. Ivanov (Dekker, New York, 1988), pp. 49–130.
[25] D. Exerowa, I. B. Ivanov, and A. Scheludko, in *Research in Surface Forces*, edited by B. V. Derjaguin (National Bureau of Standards, Washington, DC, 1964), p. 144; B. V. Toshev and I. B. Ivanov, Colloid Polym. Sci. **253**, 558 (1975); Z. M. Zorin, D. Platikanov, N. Rangelova, and A. Scheludko, in *Surface Forces and Liquid Boundary Layers*, edited by B. V. Derjaguin (Nauka, Moscow, 1983), p. 200.
[26] *Thin Liquid Films: Fundamentals and Applications* (Ref. [24]).
[27] D. Exerowa and Kruglyakov, *Foam and Foam Films* (Elsevier, Amsterdam, 1998).
[28] A. V. Neimark and M. Vignes-Adler, Phys. Rev. E **51**, 788 (1995).
[29] J. A. de Feijter and A. Vrij, J. Electroanal. Chem. Interfacial Electrochem. **37**, 9 (1972).
[30] G. F. Teletzke, H. T. Davis, and L. E. Scriven, Rev. Phys. Appl. **23**, 989 (1988).
[31] B. V. Derjaguin, V. M. Starov, and N. V. Churaev, Kolloid. Zh. **38**, 875 (1976); F. Renk, P. C. Wayner, and G. M. Homsy, J. Colloid Interface Sci. **67**, 408 (1978).
[32] A. V. Neimark and L. I. Kheifetz, Kolloid. Zh. USSR **43**, 500 (1981).
[33] I. B. Ivanov and D. S. Dimitrov, in *Thin Liquid Films: Fundamentals and Applications* (Ref. [24]), pp. 379–496.
[34] N. V. Churaev and Z. M. Zorin, Adv. Colloid Interface Sci. **40**, 109 (1992).
[35] J. R. Philip, J. Chem. Phys. **66**, 5069 (1977).
[36] M. Kagan and W. V. Pinczewski, J. Colloid Interface Sci. **180**, 293 (1995).
[37] K. J. Mysels, K. Shinoda, and S. Frankel, *Soap Films, Studies of their Thinning and a Bibliography* (Pergamon, New York, 1959).
[38] B. Levich, *Physicochemical Hydrodynamics* (Prentice-Hall, Englewood Cliffs, NJ, 1962).
[39] P. G. de Gennes, Rev. Mod. Phys. **57**, 827 (1985).
[40] J. W. Keuskamp and J. Lyklema, *Adsorption at Interfaces*, edited by K. L. Mittal, ACS Symposium Series Vol. 8 (American Chemical Society, Washington, DC, 1975), p. 191.
[41] V. Bergeron and C. J. Radke, Langmuir **8**, 3020 (1992).
[42] A. D. Nikolov, P. A. Kralchevsky, I. B. Ivanov, and D. T. Wasan, J. Colloid Interface Sci. **133**, 13 (1989).
[43] O. Krichevsky and J. Stavans, Phys. Rev. Lett. **74**, 2752 (1995).
[44] O. Belorgey and J. J. Benattar, Phys. Rev. Lett. **66**, 313 (1991); S. E. Friberg, Langmuir **8**, 1889 (1992).
[45] B. Cabane and R. Duplessix, J. Phys. (France) **48**, 651 (1987); S. Lionti-Addad and J. M. Meglio, Langmuir **8**, 324 (1992); R. Bruinsma, J. M. Meglio, D. Quere, and S. Cohen-Addad, *ibid.* **8**, 3161 (1992).
[46] J. Lucassen, *Anionic Surfactants—Physical Chemistry of Surfactant Action*, edited by E. H. Lucassen-Reynders, Surfactant Science Series Vol. 11 (Dekker, New York, 1981), p. 217; D. A. Edwards, H. Brenner, and D. T. Wasan, *Interfacial Transport Processes and Rheology* (Butterworth-Heinemann, Boston, 1991); J. B. Fournier, Phys. Rev. Lett. **75**, 854 (1995); J. C. Earnshaw and D. J. Sharpe, J. Chem. Soc., Faraday Trans. **92**, 611 (1996).
[47] H. A. Barnes, J. F. Hutton, and K. Walters, *An Introduction to Rheology*, 2nd ed. (Elsevier, Amsterdam, 1993).
[48] H. Hervet and P. G. de Gennes, C. R. Acad. Sci. URSS **229II**, 499 (1984).
[49] C. W. Park and G. M. Homsy, J. Fluid Mech. **139**, 291 (1984).
[50] *Foams: Fundamentals and Applications*, edited by R. K. Prud'homme and S. A. Khan (Dekker, New York, 1995).
[51] J. Israelachvili, *Intermolecular and Surface Forces* (Academic, London, 1992).
[52] Z. I. Khatib, G. J. Hirasaki, and A. H. Falls, SPE Reservoir Eng. **3**, 919 (1988).